

Relativistic Compton effect on the bound electron

V. G. Gorshkov, A. I. Mikhaïlov, and S. G. Sherman

Leningrad Institute of Nuclear Physics, USSR Academy of Sciences

(Submitted October 13, 1972)

Zh. Eksp. Teor. Fiz. 64, 1128-1140 (April 1973)

A formula for the cross section for photon-bound electron scattering with ionization of the atom is derived for incident photon energies much higher than the ionization energy and for small αZ . The formula is valid for any magnitude q of the momentum imparted to the nucleus, including $q \sim m$.

1. INTRODUCTION

The scattering of hard photons ($\omega \sim m$) by bound electrons is, when accompanied by ionization of the atom, maximal at small momentum transfers to the nucleus $q \sim \eta$, where $\eta = m\alpha Z$ is the mean momentum of a bound K-electron (the inverse Bohr radius of the orbit). Simmation over the domain of all q leads in the weak-coupling limit (correct to terms of order $(\alpha Z)^2$) to a cross section coincident with the cross section for the Compton effect on the free electron. It is however of interest to consider the process at large $q \sim m \gg \eta$ in the region which is kinematically inaccessible to the Compton effect on the free electron. In this region, the cross section for the process is much smaller than the cross section on the free electron and is of the order of 10^{-32} cm² for hydrogen ($Z = 1$). However, for aluminum ($Z = 13$), this cross section is already of the order of 10^{-28} cm², while for iron ($Z = 26$) it is of the order of 10^{-27} cm². Scattering of photons by bound electrons at large q has a number of distinctive features not obtaining for the free electron.

We consider only the light elements and derive the cross section in the first nonvanishing approximation with respect to $\alpha Z \ll 1$. In this approximation the amplitude of the process can be obtained with the aid of perturbation-theory diagrams (Fig. 1). The diagrams 1b and 1c include Coulomb corrections to the Green function of the intermediate electron and to the wave function of the outgoing electron, and are, generally speaking, of the order of αZ as compared to the diagram 1a which includes scattering by the free electron. When $q \sim m$, however, scattering by the free electron is kinematically impossible, and all the diagrams contain a small term of order αZ connected with the Coulomb transfer of momentum q to the nucleus. For small $q \sim \eta$ the contribution of the diagram 1a to the cross section is of the order of unity, and the amplitude computed with the aid of the diagrams of Fig. 1 will be correct to within terms of the order of $q/m \sim \alpha Z$.

For large momentum transfers $q \sim m$ to the nucleus, the entire process should take place at small distances of order of $q^{-1} \sim 1/m$ from the nucleus. The probability of finding an electron at such small distances is proportional to $|\psi(r \sim 1/m)|^2 m^{-3} \sim |\psi(r = 0)|^2 m^{-3} \sim (\alpha Z)^3$. Thus the cross section, together with allowance for the Coulomb factor αZ in the amplitude, is proportional to $r_0^2 (\alpha Z)^5$, where $r_0 = \alpha/m$ is the classical electron radius, which determines the order of magnitude of the free Compton-effect cross section.

All the computations are carried out on the basis of the electron-nucleus Coulomb interaction; this approximation is valid for one-electron atoms. At large momentum transfers $q \sim m$ the influence of the screening

by the atomic electrons is small and all the results obtained are applicable to neutral atoms with a relative accuracy of the order of (αZ) . For processes involving K-electrons, screening is small for any q .

The diagram 1c has a resonance behavior (Sec. 4) connected with the production of an almost real final electron of small virtuality $\sim \eta$ and its subsequent scattering by the Coulomb field of the same nucleus. In the region of the resonance, the factor $(\alpha Z)^2$, which arises as a result of Coulomb scattering, is cancelled out and the cross section becomes equal to the product of the Compton-effect cross section on the free electron, the Coulomb scattering cross section, and the resonance factor proportional to $|\psi(0)|^2 \sim (\alpha Z)^3$ and dependent on the state of the atomic electron. The resonance width $\sim \eta$ and therefore the total contribution of the resonance to the cross section yields a value of the order of $(\alpha Z)^4$, whereas the nonresonance part makes a contribution of the order of $(\alpha Z)^5$. As αZ increases, the contribution of the nonresonance diagrams increases and the resonance is gradually smeared out.

Diverse, simple, limiting cases can be obtained from the general formula for the differential cross section (Sec. 4).

The entire analysis of the present paper is valid for incident-photon energies ω_1 much higher than the ionization potential $\eta^2/2m$. For energies $\omega_1 \sim \eta$ the momentum transfer $q \lesssim \eta$; therefore, as has been pointed out before, the formulas are valid to within terms of the order of $\omega_1/m \sim \alpha Z$. In this case the dipole approximation is

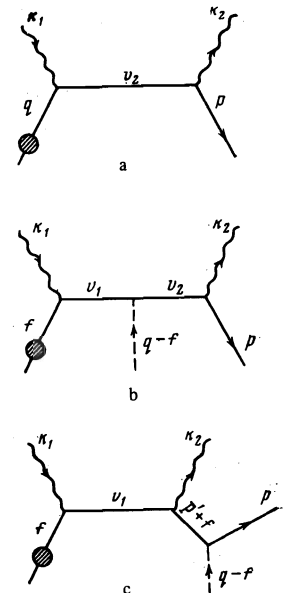


FIG. 1. Feynman diagram for the process.

inapplicable. Note that in this region the nonrelativistic Pauli approximation^[1,3] yields correctly only the zeroth (with respect to αZ) term determined by the sea-gull diagram.^[3] Terms of the order of ω_1/m that are contained in the nonrelativistic pole diagrams^[1] are an excess over the accuracy, for the relativistic correction to the dominant term is also of the order of $(E - m)/m \sim \omega_1/m$, where $E = \omega_1 + m - \eta^2/2m$ is the total energy of the system (the energy of the intermediate electron in the Dirac pole diagram in Fig. 1)^[2,3]. The low-energy theorem (terms $\sim \omega_1/m$)^[2] can be derived only on the basis of the relativistic approach. Thus, the nonrelativistic approach with allowance for higher-order terms of perturbation theory in which the perturbation is the Coulomb field is valid only in the dipole approximation, i.e., for $\omega_1 \ll \eta$. The allowance for retardation carried out in the nonrelativistic approximation^[1,4-6] is an exaggeration of the accuracy.

The Compton effect on the bound electron with ionization, when $\eta \gg \omega_1 \sim \eta^2/2m$, has been considered in a number of papers^[4,5,7]. The results of these papers are matched with the results of the present paper for $\eta \gg \omega_1 \gg \eta^2/2m$.

2. AMPLITUDE AND CROSS SECTION

Let us denote by $K_i = (\omega_i, \mathbf{k}_i)$ the momenta of the initial ($i = 1$) and final ($i = 2$) photons. $P = (\epsilon, \mathbf{p})$ is the momentum of the outgoing electron. Let us also introduce the 4-vectors:

$$Q = (m, \mathbf{q}), \quad K = K_1 - K_2 = (\omega_1 - \omega_2, \boldsymbol{\kappa}), \quad (1)$$

($h = c = 1$), where \mathbf{q} is the momentum imparted to the nucleus and $\boldsymbol{\kappa} = \mathbf{k}_1 - \mathbf{k}_2$. We shall denote the absolute values of the corresponding three-dimensional vectors by the quantities p, q , and κ . Using this notation, we can, in the approximation being used here, write the energy-momentum conservation law in the form of a single four-dimensional equation:

$$K_1 + Q = P + K_2 \quad \text{and} \quad Q = P - K. \quad (2)$$

The amplitude of the process is determined by the sum of the three Feynman diagrams (Fig. 1) and three similar diagrams with the photon lines interchanged. Therefore, it is sufficient to compute the diagrams in Fig. 1. The hatched block in Fig. 1 represents the wave function of the initial electron, which we assume for simplicity, to be a K-electron. The wave function of a K-electron in the Coulomb field has in momentum space the following form (terms of order $(\alpha Z)^2$ are discarded):^[8, 1]

$$\langle \mathbf{f} | \varphi \rangle = (1 + \mathcal{f}/2m) u_0 \langle \mathbf{f} | \varphi^0 \rangle, \quad \mathcal{f} = \alpha \mathcal{f}, \quad (3)$$

$$(1 + \mathcal{f}/2m) u_0 = u_f + O(\mathcal{f}^2/m^2),$$

where α and u_f are the Dirac matrices and bispinor for an electron with momentum \mathbf{f} , u_0 is the bispinor for an electron at rest, and $\langle \mathbf{f} | \varphi^0 \rangle$ is the nonrelativistic function of a K-electron:

$$\langle \mathbf{f} | \varphi^0 \rangle = N (-\partial / \partial \eta) \langle \mathbf{f} | V_m | 0 \rangle, \quad (4)$$

$$\langle \mathbf{f} | V_m | \mathbf{s} \rangle = 4\pi / [(\mathbf{f} - \mathbf{s})^2 + \eta^2], \quad \langle \mathbf{f} | V_m | \mathbf{s} \rangle = \langle \mathbf{f} - \mathbf{s} | V_m | 0 \rangle, \quad (5)$$

$$N = \psi(r=0) = (\eta^2/\pi)^{1/2}, \quad \eta = m\alpha Z. \quad (6)$$

The quantity (5) is the Fourier component of the Yukawa potential. The function (4) is normalized by the usual condition:

$$\int \langle \varphi^0 | \mathbf{f} \rangle \langle \mathbf{f} | \varphi^0 \rangle \frac{d^3 f}{(2\pi)^3} = 1. \quad (7)$$

The dominant contribution to the integrals (7), as to all integrals with the function (3), is made by the region $f \sim \eta$ (6). The diagram in Fig. 1a is a simple product of the diagram for the free Compton effect and the wave function (3) with the argument $\mathbf{f} = \mathbf{q}$. Its contribution I_a can be written in the form

$$I_a = 4\pi\alpha\bar{u}_p \hat{e}_2 \frac{\hat{v}_2 + m}{v_2^2 - m^2} \hat{e}_1 \langle \mathbf{q} | \varphi \rangle$$

$$= r_0 \frac{(4\pi)^2 N \eta}{a^2 a_2} \bar{u}_p \hat{e}_2 (\hat{v}_2 + m) \hat{e}_1 (\hat{Q} + m) u_0;$$

$$v_2 = K_2 + P, \quad r_0 = \alpha/m, \quad a = q^2 + \eta^2, \quad a_2 = v_2^2 - m^2,$$

$$\hat{A} = \gamma_0 A_0 - \boldsymbol{\gamma} \mathbf{A}, \quad \bar{u} u = 2m. \quad (8)$$

The vectors \mathbf{Q} and \mathbf{P} are defined in (1), \mathbf{e}_i are the photon polarizations, and \bar{u}_p and u_0 are Dirac bispinors.

In the diagram of Fig. 1a, the whole transferred momentum \mathbf{q} can be imparted to the nucleus only via the wave function of the initial electron. Therefore, for large q this diagram is small owing to the smallness of the wave function (3) when $q \sim m$. For small $q \leq \eta$ the wave function is not small and the quantity $\int d^3 q \sim r_0^2$. The second term in (3) then yields a correction of the order of αZ as compared to the first term.

In the diagrams of Figs. 1b and 1c, the whole momentum can be transferred to the nucleus via a secondary Coulomb photon, while the argument \mathbf{f} of the wave function is made small: $f \sim \eta$. The region $f \gg \eta$ makes a small contribution, on account of the decrease of the wave function. Therefore, the second term in (3) can be discarded, i.e., in the diagrams of Figs. 1b and 1c, it is sufficient to consider only the nonrelativistic wave function of the initial electron. Discarding the quantity $f \sim \eta$ in the electron propagator²⁾ of the diagram in Fig. 1b, and considering the momentum \mathbf{q} to be arbitrary, we obtain the contribution I_b of the diagram in Fig. 1b in the form

$$I_b = 4\pi\alpha\bar{u}_p \hat{e}_2 \frac{\hat{v}_2 + m}{v_2^2 - m^2} \gamma_0 \frac{\hat{v}_1 + m}{v_1^2 - m^2} \hat{e}_1 u_0 \langle \mathbf{q} | V_0 | \varphi^0 \rangle \alpha Z. \quad (9)$$

With the aid of the representation (4) and the trivial identity

$$-\frac{\partial}{\partial \eta} \int \langle \mathbf{f} | V_p | \mathbf{f}' \rangle \langle \mathbf{f}' | V_m | \mathbf{s} \rangle \frac{d^3 f'}{(2\pi)^3}$$

$$= -\frac{\partial}{\partial \eta} \langle \mathbf{f} | V_p V_m | \mathbf{s} \rangle = \langle \mathbf{f} | V_{p+m} | \mathbf{s} \rangle$$

we obtain

$$\langle \mathbf{q} | V_p | \varphi^0 \rangle = N \langle \mathbf{q} | V_{p+m} | 0 \rangle. \quad (10)$$

Substituting (10) into (9) and setting $\mathbf{p} = 0$, we finally obtain for I_b :

$$I_b = r_0 \frac{(4\pi)^2 N \eta}{a a_1 a_2} \bar{u}_p \hat{e}_2 (\hat{v}_2 + m) \gamma_0 (\hat{v}_1 + m) \hat{e}_1 u_0;$$

$$v_1 = K_1 + M, \quad a_1 = v_1^2 - m^2 = 2m\omega_1, \quad M = (m, 0, 0, 0) \quad (11)$$

In the diagram of Fig. 1c, the small three-dimensional vector $\mathbf{f} \sim \eta$ can also be discarded in the numerators of the electron propagators and in the denominator of the electron propagator coupling the photons of momenta \mathbf{k}_1 and \mathbf{k}_2 . The denominator of the second electron propagator can however be small, and therefore, we cannot discard the vector \mathbf{f} in it. Noting that this denominator can be written in the form

$$\frac{1}{(\mathbf{f} + \boldsymbol{\kappa})^2 - p^2} = \frac{1}{4\pi} \langle -\boldsymbol{\kappa} | V_p | \mathbf{f} \rangle \quad (12)$$

and using Eq. (10), we obtain for the contribution of the diagram c the following expression

$$I_c = 4\pi\alpha\bar{u}_p\gamma_0(\hat{P}' + m)\hat{e}_2\frac{\hat{v}_1 + m}{v_1^2 - m^2}\hat{e}_1u_0\langle -\kappa | V_p | \varphi^0 \rangle \frac{\alpha Z}{q^2} \quad (13)$$

$$= r_0 \frac{(4\pi)^2 N \eta}{q^2 a_3} \bar{u}_p \gamma_0 (\hat{P}' + m) \hat{e}_2 (\hat{v}_1 + m) \hat{e}_1 u_0,$$

$$P' = P - Q + M = (\varepsilon, \kappa), \quad a_3 = \kappa^2 - (p + i\eta)^2. \quad (14)$$

The sum of (8), (11), and (13), together with the cross-symmetric diagrams, leads to the following expression for the amplitude A of the process³⁾:

$$A = r_0 (4\pi)^2 N \eta a^{-1} \bar{u}_p F u_0; \quad (15)$$

$$F = \{L_1 \hat{e}_2 (\hat{v}_2 + m) \hat{e}_1 (\hat{Q} + m) + L_2 \hat{e}_2 (\hat{v}_2 + m) \gamma_0 (\hat{v}_1 + m) \hat{e}_1 + L_3 \gamma_0 (\hat{P}' + m) \hat{e}_2 (\hat{v}_1 + m) \hat{e}_1 + (K_2 \hat{z} - K_1, e_2 \hat{z} e_1)\} \times (1 + O(\alpha Z q^2 / m^2, \alpha^2 Z^2)), \quad (16)$$

$$L_1 = 1 / a a_3, \quad L_2 = 1 / a_1 a_2, \quad L_3 = 1 / a_1 a_3;$$

$$a = q^2 + \eta^2, \quad a_1 = 2m\omega_1, \quad a_2 = v_2^2 - m^2, \quad a_3 = \kappa^2 - (p + i\eta)^2, \\ v_1 = K_1 + M, \quad v_2 = P + K_2, \quad P' = P - Q + M, \quad M = (m, 0, 0, 0).$$

The differential cross section for the process averaged over the initial and summed over the final photon and electron polarizations ν and λ respectively can be expressed in terms of the amplitude A in the form

$$d\sigma = \frac{1}{2m2\omega_1} \frac{1}{4} \sum_{\nu, \lambda} |A|^2 \frac{d^3 p}{2\varepsilon (2\pi)^3} \frac{d^3 k_2}{2\omega_2 (2\pi)^3} 2\pi \delta(\omega_1 + m - \varepsilon - \omega_2) \\ = r_0^2 \frac{1}{2\pi^2} \frac{\eta^2}{a^2} \frac{1}{\omega_1 \omega_2 \varepsilon} J d\Gamma; \quad (17)$$

$$d\Gamma = d^3 p d^3 k_2 \delta(\omega_1 + m - \varepsilon - \omega_2), \quad (18)$$

$$J = \frac{1}{4m} \sum_{\nu, \lambda} |\bar{u}_p F u_0|^2 = \frac{1}{4} \sum_{\nu_1, \nu_2} \text{Sp} F(\gamma_0 + 1) \bar{F}(p + m), \quad \bar{F} = \gamma_0 F^\dagger \gamma_0.$$

The expression for J has the form

$$\begin{aligned} \frac{1}{4} J = & 2L_1^2 \{q^2 [PK_2(\omega_2 - 4) - E] + 4[PK_2(1 + PK_1) + 1]\} \\ & + 4L_2^2 \{(\omega_1 - 1)[PK_2(k_2 k_1 + \omega_2 \omega_1) + QK_1 - 2\omega_1 E] + \varepsilon PK_2 \\ & + 2E\} + 4|L_3|^2 \{K_2 K_1 [(\omega_1 - 1)(pk_2 + \varepsilon \omega_2) - \varepsilon \omega_1 - 3\omega_1 - 1] \\ & + PK_2(\omega_1^2 + \omega_2 + 1) - PK_1(\omega_2 \omega_1 + E) + \varepsilon E(1 + E) + \omega_1(\omega_1 - 1) \\ & + 2\varepsilon(\varepsilon - 1)(E + \omega_2)\} + L_1 M_1 \{q^2 [(\varepsilon - 1)q^2 + 3K_2 K_1 - 4] \\ & + 4(K_2 K_1 + 2)\} + 2L_2 M_2 \{(k_2 k_1)^2 + (3 + \varepsilon^2 - 2\varepsilon)(k_2 k_1) \\ & + \varepsilon[2(pk_2)(pk_1) + (2 - \omega_1)pk_2 - (2 + \omega_2)pk_1 + 6\varepsilon - 2] \\ & + \omega_2 \omega_1(\varepsilon^2 - \omega_2 \omega_1 - 6\varepsilon + 1)\} + 2(L_3 M_3) \{(\varepsilon^2 - \varepsilon + p\kappa)[2(\varepsilon - 1)K_2 K_1 \\ & - 2\varepsilon^2 + 5\varepsilon - 1] + (2\varepsilon + 1)(K_2 K_1)^2 - (2\varepsilon^2 - \varepsilon + 1)K_2 K_1 + \varepsilon^2 + 4\varepsilon - 1\} \\ & + 4L_1 L_2 \{PK_1[E(PK_2) + \omega_2 PK_1 - (\varepsilon + 2)K_2 K_1 + 2\omega_2 \omega_1 + 2\omega_1 - 3\omega_2] \\ & + 2(QK_1 - \omega_1^2 + 2E)\} + 4L_1 M_2 \{\omega_2(PK_1)^2 - \omega_1(PK_2)^2 + PK_2[(\varepsilon + 1)QK_1 \\ & - 2QK_2 + E\omega_1 + 2\varepsilon\omega_2] - PK_1(\varepsilon K_2 K_1 + \omega_2 \omega_1 + 2\varepsilon E) - E(1 + \varepsilon + 4\omega_2)K_2 K_1 \\ & - 2\omega_2 Q^2 - \omega_2 \omega_1 + 4\varepsilon\} + 4\text{Re}(L_1 L_2) \{PK_2[E(PK_2) - \omega_2 PK_1 - \varepsilon K_2 K_1 \\ & + (\omega_1 - 1)(4\varepsilon + \omega_1) - \omega_2(2\varepsilon + 1)] + K_2 K_1 \varepsilon(6 + 2\omega_2 - 5\omega_1) \\ & - PK_1(Q^2 + \omega_1^2 + \varepsilon \omega_1 + 2\varepsilon^2 - 6\varepsilon - 3E) + 4\varepsilon E + 2\omega_2(\varepsilon - 1) + \omega_1(\omega_2 - 2)\} \\ & + 4\text{Re}(L_1 M_3) \{PK_2(2\varepsilon K_2 K_1 + 2PK_2 - QK_1 + \varepsilon \omega_1 - 2\varepsilon^2 - 5\varepsilon - 1) \\ & + K_2 K_1(\varepsilon^2 + 2\varepsilon - \omega_2 + 3) + PK_1(2\varepsilon - 2\omega_2 - \varepsilon \omega_2) \\ & + (K_2 K_1)^2 + \omega_2 \omega_1 Q^2 + \varepsilon(6\omega_1 - \omega_2 + 4 - 2\varepsilon \omega_1) + 3\omega_2\} \\ & + 4\text{Re}(L_2 L_3) \{(\omega_1 - 1)[(PK_1)Q^2 + 2\varepsilon(\varepsilon - 1)QK_1 \\ & + 2(E\omega_1 PK_1 - \varepsilon \omega_1 PK_2 + E\varepsilon K_2 K_1 - \omega_2 \omega_1) + \omega_1] \\ & + \omega_1(\omega_2 PK_1 - \omega_1 PK_2 - \varepsilon K_2 K_1 + \varepsilon) + E(PK_1) - PK_2 - 2\omega_2 \\ & + 2\varepsilon(1 + E^2 + \omega_2 E)\} + 4\text{Re}(L_2 M_3) \{(2\varepsilon^2 - PK_1)(\varepsilon K_2 K_1 + \omega_1 PK_2 \\ & - \omega_2 PK_1) + K_2 K_1(2PK_2 + 2\omega_2 - 3\varepsilon - \varepsilon E) + PK_1(PK_2 + \varepsilon \omega_1 + E\omega_1 - 2E) \\ & - PK_2(E^2 + \varepsilon E + \varepsilon \omega_1 + \omega_1) + \omega_2(2\varepsilon^2 + 3\omega_2 - \omega_1) \\ & + 4\varepsilon E(\varepsilon + \omega_1 - \varepsilon \omega_1)\} + \{(\omega_2, k_2) = (-\omega_1, -k_1)\}. \end{aligned} \quad (19)$$

Here

$$m = 1, \quad E = 1 + \omega_1 = \varepsilon + \omega_2, \quad AB = a_0 b_0 - \mathbf{ab}, \\ P = (\varepsilon, \mathbf{p}), \quad K_2 = (\omega_2, \mathbf{k}_2), \quad K_1 = (\omega_1, \mathbf{k}_1), \quad Q = (m, \mathbf{q}), \\ K = (\omega_1 - \omega_2, \kappa), \quad \kappa = \mathbf{k}_1 - \mathbf{k}_2, \quad Q = P + K_2 - K_1, \quad K = K_1 - K_2, \\ M_1(\omega_1, \omega_2, \mathbf{k}_1, \mathbf{k}_2) = L_1(-\omega_2, -\omega_1; -\mathbf{k}_2, -\mathbf{k}_1).$$

The above-cited formula has been verified by us by going over to the numerous limiting cases obtained in Sec. 4 by other methods.

3. KINEMATICS

For small $q \sim \eta$ the dominant term in the amplitude (15) and (16) will be the first term containing a a^{-2} . For large $q \sim m$ the dominant term will be the third term containing, for $|\kappa - p| \sim \eta$, the factor a_3^{-1} . To separate out the resonance region, we must go over to new variables that fix the quantities q , κ , and p .

The process under study is, as can be seen from the diagrams of Fig. 1, equivalent to a process with five initial and final particles, and has five independent variables. These five variables are ω_1 and the four independent variables entering into $d\Gamma$ in (18). One of the azimuthal angles entering into $d\Gamma$ corresponds to a rigid rotation of the whole system of vectors \mathbf{k}_1 , \mathbf{k}_2 , and \mathbf{p} , which are fixed relative to each other; it does not enter into the amplitude. The differential with respect to this angle can, after averaging over all the polarizations, be replaced by 2π . Selecting as such an angle the azimuthal angle of the vector \mathbf{k}_2 and going over from the polar angle to the variable κ , we obtain

$$d\Omega_{k_2} = 2\pi \kappa d\kappa / \omega_1 \omega_2.$$

To select the remaining variables, let us consider the system of coordinates shown in Fig. 2, with the Z axis directed along the vector $-\kappa$, and the vectors \mathbf{k}_1 and \mathbf{k}_2 lying in the XZ plane. In this system, for fixed magnitudes of the vectors q , κ , and p , the rigid triangle formed by these vectors can rotate through an arbitrary angle $0 \leq \varphi \leq 2\pi$ about the Z axis. Using as the three remaining independent variables the quantities p , q , and φ , we obtain

$$d^3 p = \frac{pq}{\kappa} dp dq d\varphi.$$

For a fixed value of p , the energy δ -function in (18) is removed with a unit Jacobian by the differential $d\omega_2$, and we finally obtain

$$d\Gamma = 2\pi \frac{qp\omega_2}{\omega_1} d\kappa dq dp d\varphi. \quad (20)$$

On the angle φ depend, as can be seen from Fig. 2, only the scalar products $\mathbf{p} \cdot \mathbf{k}_1$, $\mathbf{p} \cdot \mathbf{k}_2$, $\mathbf{q} \cdot \mathbf{k}_1$, and $\mathbf{q} \cdot \mathbf{k}_2$. However, the analytical integration with respect to this angle considerably complicates the formula (19). Let us also write out the phase volume in the variables Ω_{k_2}

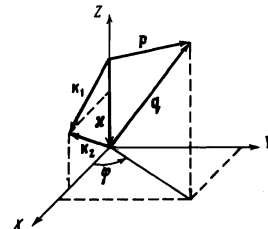


FIG. 2

and q . Before integrating the energy δ -function with respect to $d\omega_2$ in (18), we can replace d^3p by d^3p . For fixed Ω_{k_2} and q the momentum p depends on ω_2 . Therefore, there appears a Jacobian in the integration of the energy δ -function with respect to $d\omega_2$, and the phase volume (18) assumes in terms of these variables the form

$$d\Gamma = \frac{\omega_2^2 \varepsilon}{m\omega_1 - qk_1 - q^2/2} d\Omega_{k_2} d^3q \cong d\Gamma_0 d^3q \left(1 + \frac{qk_1}{m\omega_1}\right) + O\left(\frac{q^2}{m^2}\right), \quad (21)$$

$$d\Gamma_0 = \frac{\omega_2^2 \varepsilon}{m\omega_1} d\Omega_{k_2}.$$

The physical region of the variables p and κ for a fixed ω_1 and different q is limited by the conditions:

$$|q - p| \leq \kappa \leq q + p, \quad \varepsilon - m = \omega_1 - \omega_2 \leq \kappa \leq \omega_1 + \omega_2 = 2\omega_1 + m - \varepsilon, \\ \varepsilon^2 = p^2 + m^2.$$

In Fig. 3 are drawn three straight lines: $\kappa = p + q$, $\kappa = p - q$, $\kappa = q - p$, and two hyperbolas: $\kappa = \varepsilon - m$, $\kappa = 2\omega_1 + m - \varepsilon$. The physical region, which is the region enclosed by these curves, is hatched. For $q = 0$ the straight lines $\kappa = p + q$ and $\kappa = p - q$ coincide, and the physical region degenerates into the straight line $\kappa = p$ with the maximum momentum $p = p_0 = \mathcal{P}_0(0)$, where

$$\mathcal{P}_0(q) = \frac{(2\omega_1 + q)(2\omega_1 + 2m + q)}{2(2\omega_1 + m + q)}.$$

The value p_0 coincides with the maximum electron momentum in the free Compton effect. As q increases, the maximum value of the momentum $p_0(q)$ increases and attains the point of intersection of the two hyperbolas with the value $p = p_{\max} = (\omega_1(\omega_1 + 2m))^{1/2}$ when $q = q_0 = p_{\max} - \omega_1$. When $q > q_0$ the curve $\kappa = p - q$ ceases to be a boundary of the physical region. The value $\omega_2 = 0$ corresponds to $p = p_{\max}$. These values of the variables are attained only when $q > q_0$. For $q < q_0$ there exists a minimum ω_2 :

$$\omega_{2\min} = \mathcal{P}_0(q) - q - \omega_1.$$

The resonance region $|\kappa - p| \sim \eta$ corresponds to the nearest vicinity of the straight line $\kappa = p$. The regions $p < q/2$ and $p > p_0$ lie below and above the curve $\kappa = p$. Therefore in these regions a resonance in the amplitude cannot arise on $\kappa = p$. This is natural, since the section of the resonance diagram in Fig. 1c located to the left of the pole term with momentum p is the amplitude of the free Compton effect, for which the maximum momentum is p_0 , while the minimum

$$p_{\min} = |\kappa + q|_{\min} = q/2 \quad \text{for } \kappa = p_{\min}.$$

Thus, the regions $p < q/2$ and $p > p_0$ make a contribution of the order of $(\alpha Z)^5$ to the amplitude, while the con-

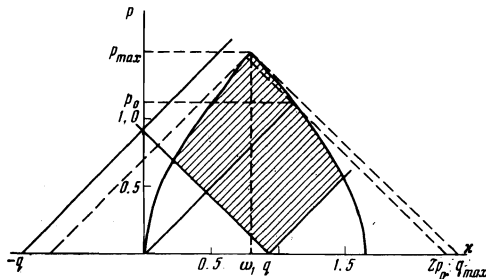


FIG. 3. The physical region (hatched) of variation of the variables, $m = 1$.

tribution of the entire remaining region, which contains the resonance, is of the order of $(\alpha Z)^4$.

For $q > 2\omega_1$ there arises a minimum momentum value equal to $p_{\min} = -\mathcal{P}_0(-q) > 0$. For $q \geq 2p_0$ the entire physical region is located in the region $p \geq p_0$, where there is no resonance. Therefore, the cross section is of the order of $(\alpha Z)^5$ when $q > 2p_0$. In the region $q \sim 2p_0$ the cross section $d\sigma/dq$ should drop from a value of the order of $(\alpha Z)^4$ for $q < 2p_0$ to a value $\sim (\alpha Z)^5$ for $q > 2p_0$.

4. ASYMPTOTIC FORMULAS FOR THE CROSS SECTION

1. The region of small momentum transfers q :

$$q \ll p = \kappa, \quad p \gg \eta, \quad \omega_1 \gg \eta^2/2m, \quad 0 \leq \varphi \leq 2\pi. \quad (22)$$

In this region the dominant term is the diagram of Fig. 1a, i.e., the amplitude (8), or the first term in the amplitude (16). The diagram of Fig. 1a, (8), is the product of the nonrelativistic wave function of the bound electron $\langle q | \varphi^0 \rangle$ and the amplitude of the Compton effect on an electron with the initial momentum q . The latter factor contains linear correction terms of the order of q/m , the neglect of which leads to the standard impulse approximation. Furthermore, the linear terms of the order of q/m arise from the wave function of the final electron and are contained in the diagram of Fig. 1c, (13).

Thus, in terms of the variables of (21), and up to linear terms of the order of (q/m) , the expression for the cross section has the form

$$d\sigma = \frac{QK_1}{m\omega_1} |\langle \varphi^0 | q \rangle|^2 \frac{d^3q}{(2\pi)^3} d\sigma_q \left(1 - \frac{\varepsilon}{m} \frac{\kappa q}{\kappa^2} \frac{q^2 + \eta^2}{(nq)^2 + \eta^2}\right) \left(1 + O\left(\frac{q^2}{m^2}\right)\right), \quad (23)$$

where $n = \kappa/\kappa$ and $d\sigma_q$ is the cross section for the free Compton effect on an electron with the initial momentum q . The latter factor arose from the wave function of the final-state electron.

Expanding (23) in powers of q and retaining only the linear terms, we obtain

$$d\sigma = |\langle \varphi^0 | q \rangle|^2 \frac{d^3q}{(2\pi)^3} d\Omega_{k_2} \left\{ \sigma_0 \left(1 - \frac{\varepsilon}{m} \frac{\kappa q}{\kappa^2} \frac{q^2 + \eta^2}{(nq)^2 + \eta^2}\right) + \frac{qk_1}{m\omega_1} - a_1 \frac{qk_1}{m\omega_1} - a_2 \frac{qk_2}{m\omega_2} \right\}, \quad (24)$$

$$a_1 = \omega_1 \frac{\partial}{\partial \omega_1} \left(\frac{\omega_1^2}{\omega_2^2} \sigma_0 \right), \quad a_1(\omega_1, \omega_2) = \frac{r_0^2}{2} \left\{ \frac{\omega_1}{\omega_2} - \frac{\omega_2}{\omega_1} - 2 \frac{m}{\omega_1} \left(1 + \frac{m}{\omega_1} - \frac{m}{\omega_2}\right) \right\}, \quad a_2 = a_1(-\omega_2, -\omega_1),$$

where $d\sigma_0 = \sigma_0 d\Omega_{k_2}$ is the differential cross section for the free Compton effect on an electron with zero initial momentum:

$$\sigma_0 = \frac{d\sigma_0}{d\Omega_{k_2}} = \frac{r_0^2}{2} \left(\frac{\omega_2}{\omega_1} \right)^2 \left\{ \frac{\omega_1}{\omega_2} + \frac{\omega_2}{\omega_1} + \left(\frac{m}{\omega_1} - \frac{m}{\omega_2} \right)^2 + 2 \left(\frac{m}{\omega_1} - \frac{m}{\omega_2} \right) \right\}. \quad (25)$$

Upon integration of (24) over the angular variables, the terms linear in q vanish, and we obtain

$$d\sigma = \frac{32}{\pi} \frac{\eta^2 q^2 dq}{(q^2 + \eta^2)^2} \sigma_0^{\text{tot}}(\omega_1) \left[1 + O\left(\frac{q^2}{m^2}\right) \right], \quad (26)$$

where $\sigma_0^{\text{tot}}(\omega_1)$ is the total cross section for the free Compton effect. After integrating (24) with respect to d^3q , we find $d\sigma$ to be coincident, on account of (7), with $d\sigma_0$ when terms of the order of $(\alpha Z)^2$ are discarded.

The formula (26) is for an initial electron in the 1s state. In the region $\eta \ll q \ll m$ formula (26) remains

valid for states with arbitrary quantum numbers n and l , upon the replacement of η by $\eta_n = \eta/n$ and the multiplication of (26) by the factor $(\eta_n/q)^2 l$.

2. Region of resonance behavior:

$$|\kappa - p| \sim \eta, \quad q/2 \leq p \leq p_0, \quad q \gg \eta, \quad 0 \leq \varphi \leq 2\pi. \quad (27)$$

In this region the dominant term is the diagram of Fig. 1c—the third term (13) in the amplitude (16). The resonance behavior is due to the fact that the energy and momentum of the second intermediate electron line in Fig. 1c are fixed by the external variables κ and p up to terms of the order of $f \sim \eta$:

$$E' = (p^2 + m^2)^{1/2}, \quad p' = \kappa.$$

Therefore, for $|p - \kappa| \sim \eta$ this intermediate electron becomes almost real, while the corresponding propagator becomes a large quantity $\sim \eta^{-1}$.

This phenomenon always arises when some term of the amplitude of the process can be split into two blocks which are amplitudes of real processes and which are connected by one line. Such a situation obtains for “three-three particle” transitions, as well as for “two-three particle” transitions if one of the initial particles is unstable.^[10] If by change the initial particles figuring in the various blocks are not bound, then the “resonance” is infinite, the amplitude is indeterminate, and the cross section depends on the laboratory conditions. In scattering on weakly bound systems there arises a resonance of width of the order of the binding momentum if the coordinate wave function does not have singularities in the vicinity of the origin and depends only on the radius $a = \eta^{-1}$ of the system, a situation which obtains in our case (the third particle here is the nucleus). In the presence of a singularity of the coordinate wave function at the origin, there arises, instead of a pole singularity, the well-known logarithmic singularity (see (29) below).

Let us set $\kappa = p$ in all the terms in (13) (in the residues at the pole) except the resonance (pole) term a_3^{-1} ,

$$\hat{P}' + m = \sum_{\lambda} u_{\lambda}^{\lambda} \bar{u}_{\lambda}^{\lambda}, \quad P' = (\varepsilon, \kappa),$$

where u_{λ}^{λ} is the Dirac bispinor with polarization λ , we can rewrite (13) in the form

$$I_c = \langle -\kappa | V_p | \varphi_{n'} \rangle A_{\lambda}^{\varepsilon} A_{\lambda}^0 / 4\pi, \quad (28)$$

$$\langle -\kappa | V_p | \varphi_{n'} \rangle / 4\pi = N / a_3, \quad a_3 = 2p(\kappa - p - i\eta), \quad (29)$$

where $A_{\lambda}^{\varepsilon}$ and A_{λ}^0 are the Coulomb-scattering and free-electron Compton-effect amplitudes, connected by the net polarization λ of the intermediate electron:

$$A_{\lambda}^{\varepsilon} = 4\pi\alpha Z \bar{u}_{\lambda} \gamma_0 u_{\lambda}^{\lambda} q^{-2}, \quad A_{\lambda}^0 = 4\pi\alpha u_{\lambda}^{\lambda} \hat{\varepsilon}_z \frac{\hat{v}_1 + m}{v_1^2 - m^2} \hat{\varepsilon}_1 u_{\lambda}. \quad (30)$$

Using the nondependence of the Coulomb scattering in the Born approximation on the polarization λ and the expressions (20), (25), (28), and (30), we obtain the cross section in the region (27) in the form

$$d\sigma = R_{nl}(\kappa, p) \frac{d\kappa}{2\pi} d\sigma_c d\sigma_C \left[1 + O\left(\frac{\kappa - p}{p}\right) \right]; \quad (31)$$

$$R_{nl} = \frac{p^2}{4\pi^2} |\langle -\kappa | V_p | \varphi_{n'} \rangle|^2, \quad R_{10} = \frac{N^2}{(\kappa - p)^2 + \eta^2}, \quad N^2 = \frac{\eta^4}{\pi}, \quad (32)$$

$$d\sigma_c = \sigma_c 2\pi \frac{mp dp}{\omega_c \varepsilon}, \quad d\sigma_C = \sigma_C 2\pi \frac{q dq}{p^2}, \quad (33)$$

$$\sigma_c = \frac{d\sigma_c}{d\Omega_p} = \frac{(2e\alpha Z)^2}{q^4} \left(1 - \frac{q^2}{4\varepsilon^2} \right), \quad \varepsilon = \omega_1 + m - \omega_2, \quad p^2 = \varepsilon^2 - m^2,$$

where σ_0 and σ_C are the differential cross sections per unit solid angle for the free Compton effect and Coulomb scattering in the Born approximation; σ_0 is determined by formula (25).

As can be seen from (31), (32), and (33), the cross section depends only on the variables ω , p , q , and κ , and, what is more, the entire dependence on κ is concentrated in the factor (32) (see (29) and (13)). The dependence on the fifth variable φ in the region (27) disappears dynamically, and, therefore, $d\varphi$ is replaced in (31) and (33) by 2π .

The cross section (31) depends on the state of the initial electron through the resonance factor R_{nl} (32). In the case of an initial electron in the 1s state, R_{10} has the standard Breit-Wigner form (32). In the case of the 2p state this factor has the form of a resonance at a pole of order 2:

$$R_{21} = \frac{N_2^2 \eta^2}{[(\kappa - p)^2 + \eta_2^2]^2}, \quad N_2^2 = \frac{\eta^2}{\pi}, \quad \eta_2 = \frac{\eta}{2}. \quad (34)$$

In the general case the expression for R_{nl} is rather unwieldy, but in the region $\eta \ll |\kappa - p| \ll m$ the quantity R_{nl} has the simple form:

$$R_{nl} = \frac{N_n^2}{(\kappa - p)^2} \left(\frac{\eta_n^2}{(\kappa - p)^2} \right)^l, \quad \eta_n = \frac{\eta}{n}. \quad (35)$$

Thus, from the shape of the peaks in the region $|\kappa - p| \sim \eta$, as in the case of the region of small $q \ll m$, we can determine the quantum numbers of the initial electron.

The formulas (31) and (24) are valid for any process involving a bound electron, with $d\sigma_0$ equal to the corresponding cross section for the free electron. The formula (31) has a simple meaning. Notice that

$$\frac{d\kappa}{2\pi\kappa^2} \sim dr, \quad N^2 = \frac{1}{V}, \quad V = \pi a^3,$$

where $a = \eta^{-1}$ is the Bohr radius, V is the volume occupied by the bound electron (volume of the atom), and r is the path traversed by the electron between the Compton and Coulomb interactions. Then (31) can be written in the form $\sigma = \sigma_0 \sigma_C r / V$. The cross section σ is the cross section for a double interaction of an electron first with a photon and then with the Coulomb field of the nucleus. The probability of such an interaction is equal to the product of the probabilities of each of the interactions, while the cross section is equal to the product of the cross sections for one of the interactions and the probability of the second. The probability of the latter is equal to the ratio of the volume of a cylinder of cross section σ_C and length r cut out from the entire volume V occupied by the electron to the volume V . Far from a resonance $r \sim 1/m$. A resonance develops in the sense that the electron is able to traverse before the second interaction a distance r of the order of the dimension a of the atom (i.e., $r \sim a$). In this case the probability of the second interaction is proportional to the ratio of the cross section σ_C for the interaction to the cross section $S = \pi a^2$ of the atom, and $\sigma = \sigma_0 \sigma_C / S$. Note that $V \sim n^3$ and $S \sim n^2$, where n is the principal quantum number of the bound electron. Therefore, as n increases, the cross section σ decreases, becoming zero as $n \rightarrow \infty$. This corresponds to the absence of the effect on a single free electron occupying the macroscopic (normalization) volume V .

In real targets there is a finite density of atoms $n_0 = L^{-3}$, where L is the interatomic distance. There-

fore, as the virtuality $|\kappa - p|$ of the electrons decreases right up to values of the order of the inverse interatomic distances: $|\kappa - p| \sim L^{-1}$, scattering of the outgoing electrons by neighboring atoms begins. The magnitude of the cross section for this process is determined by the formula $\sigma = \sigma_0 n_0 l \sigma_C = \sigma_0 \sigma_C l / L^3$, where l is the target thickness. For solid targets this value turns out to be larger than the integrated cross section (31). However, the cross section with scattering of the outgoing electron by the neighboring atoms does not depend on the state of the initial electron and is confined in a considerably narrower peak for a varying κ and a fixed p than the cross section (31), since $\eta = a^{-1} \gg L^{-1}$. Therefore, when the energy resolution is good, i.e., $\Delta \ll \eta$, the process with scattering by neighboring atoms (multiple scattering) can easily be separated from the process with scattering of the outgoing electron by "its own atom" (31).

Integrating formula (31) over κ , we obtain a cross-section distribution over the p and q variables that determines the central portion of the cross section in the plot of Fig. 4:

$$\frac{d\sigma}{dq dp} = 2\pi\eta^2 \sigma_0 \sigma_C \frac{mq}{\omega_2^2 \epsilon p}, \quad \frac{q}{2} \leq p \leq p_0. \quad (36)$$

Notice that only the lowest order diagram, Fig. 1c, of the perturbation theory has a resonance behavior connected with the presence of the pole a_3^{-1} in the amplitude (13). When all the subsequent approximations (with respect to the Coulomb field) to the wave function of the final electron are taken into account the pole is converted into a branch point of the form $a_3^{-1} - i\xi$ (see^[8]). The diagrams containing the corrections to both the wave function of the final electron and the electron Green function (for example, the combination of the diagrams in Figs. 1b and 1c) do not, in general, contain singularities in the neighborhood of $|\kappa - p| \sim \eta$ and do not have a resonance behavior. As Z grows, these diagrams begin to play a greater and greater role and the resonance is washed out.

3. The region of low ω_2 :

$$\omega_2 \ll \omega_1, \quad \kappa \approx \omega_1, \quad p \approx p_{\max}, \quad q > p_{\max} - \omega_1, \quad \omega_1 \gg \eta^2 / 2m. \quad (37)$$

This is the infrared region, where the dominant terms are the diagrams of Figs. 1a and 1b, which contain the pole $1/\omega_2$, owing to the emission of the outgoing photon from the final-electron line. The cross diagrams in this case are small, but they play an important role when gauge invariance is used, for example, in the summation

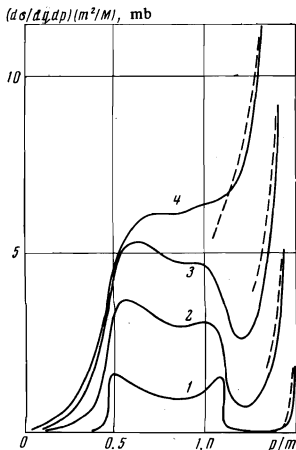


FIG. 4. Plot of the dependence of the cross-section distribution $d\sigma/dqdp$ on p for an initial electron in the 1s state for $\omega_1 = 0.806m$, $q = 0.925m$, and $p_0 = 1.115m$: for the curves 1— $Z = 1$, $M = 10^5$; 2— $Z = 13$, $M = 10$; 3— $Z = 26$, $M = 1$; 4— $Z = 50$, $M = 10^{-1}$. The dashed curves have been constructed in the region $p \sim p_{\max}$ from the infrared formula (40).

over the photon polarizations. The cross section for the process in this region is represented in the form of a product of the cross section $d\sigma_f$ for the photoelectric effect and the probability dW_γ for the accompanying radiation. As can be seen from Fig. 3, low values of ω_2 are possible only when $q > q_0 = p_{\max} - \omega_1$, where q_0 is the smallest possible value of the momentum transferred in the photoelectric effect. The cross section summed over the photon polarizations has the form

$$d\sigma = d\sigma_f dW_\gamma, \quad (38)$$

$$d\sigma_f = \sigma_f d\Omega_n, \quad \sigma_f = r_0 \frac{(2\eta)^3 p_{\max}^3}{\omega_1 q^8} \sin^2 \theta_1 \left(1 + \frac{\omega_1 - m}{4m^2} q^2 \right), \quad (39)$$

$$\sin^2 \theta_1 = 1 - (n\eta)^2, \quad \mathbf{q} = \mathbf{p}_{\max} - \mathbf{k}_1,$$

$$dW_\gamma = \frac{\alpha}{(2\pi)^2} \frac{p_{\max}^2 - (\mathbf{p}_{\max} \mathbf{n}_2)^2}{(\epsilon_{\max} - (\mathbf{p}_{\max} \mathbf{n}_2))^2} d\Omega_{k_2} \frac{d\omega_2}{\omega_2},$$

$$\mathbf{n}_i = \mathbf{k}_i / \omega_i, \quad \mathbf{n} = \mathbf{p}_{\max} / p_{\max}, \quad p_{\max} = (\omega_1(\omega_1 + 2m))^{1/2}, \quad \epsilon_{\max} = \omega_1 + m.$$

Integrating dW_γ over the angular variables and going over to the variables q and p , we obtain the following cross-section distribution over the p and q variables (see Fig. 4):

$$d\sigma / dq dp = \sigma_f W_\gamma 2\pi q / \omega_1 \omega_2 \epsilon_{\max},$$

$$W_\gamma = \omega_2 \frac{dW_\gamma}{d\omega_2} = \frac{\alpha}{\pi} \left(\frac{\epsilon_{\max}}{2p_{\max}} \ln \frac{\epsilon_{\max} + p_{\max}}{\epsilon_{\max} - p_{\max}} - 1 \right); \quad (40)$$

$$m \gg \omega_2 = \epsilon_{\max} - \epsilon \gg \Delta,$$

where Δ is the resolution in the measurement of the photon energy.

4. The region of small p :

$$\eta \ll p \ll q \approx \kappa, \quad \omega_2 = \omega_1 \gg \eta^2 / 2m, \quad 0 \leq \varphi \leq 2\pi. \quad (41)$$

In this case all the three diagrams in Fig. 1 are of the same order when $q \sim m$. When $q \ll m$ the diagram in Fig. 1b should be discarded in comparison with the diagrams in Figs. 1a and 1c. The cross section for the process in the region (41) differs from the photon-K-electron elastic scattering cross section,^[3] in that the phase volume of the final bound electron N^2 , (6), is replaced by the phase volume of the outgoing electron $d^3p / (2\pi)^3$:

$$d\sigma = d\sigma_{el} \frac{1}{N^2} \frac{d^3p}{(2\pi)^3}, \quad (42)$$

$$d\sigma_{el} = \frac{r_0^2}{2} \left(\frac{4\eta}{q} \right)^8 \left\{ (1 + \cos^2 \theta) + \frac{q^2}{2m^2} - \frac{q^2}{4m^2} \left(1 - \frac{q^2}{8m^2} \right) (1 + \cos \theta)^2 \right\} d\Omega_{k_2},$$

where $\cos \theta = \mathbf{k}_1 \cdot \mathbf{k}_2 / \omega_1 \omega_2$.

5. The region of small q and p :

$$\eta \ll q \sim p \sim \kappa \ll m, \quad \omega_1 \gg \eta^2 / 2m, \quad 0 \leq \varphi \leq 2\pi, \quad (43)$$

$$d\sigma = |\langle \mathbf{q} | \varphi^0 \rangle|^2 \left| 1 + \frac{a}{a_3} \right|^2 \frac{d^3p}{(2\pi)^3} d\sigma_T = \frac{8}{\pi^2} \frac{\eta^5}{q^8} \left| 1 + \frac{q^2}{a_3} \right|^2 d^3p d\sigma_T. \quad (44)$$

Here

$$d\sigma_T = 1/2 r_0^2 (1 + \cos^2 \theta) d\Omega_{k_2}$$

is the Thomson cross section, and a_3^3 and a are defined in (16). If $q \ll p$, then $a/a_3 \ll 1$, and (44) becomes the dominant term in (24) when $p \ll m$. If $p \ll q$, then $a_3 = a$, and (44) goes over into (42) when $q \ll m$. Let us note an interesting equality that follows from (44):

$$d\sigma / d^3p |_{p \ll q} = 4d\sigma / d^3p |_{q \ll p}.$$

We also derived the formulas (24), (31), (38), (39), (42), and (44) from the general formula (19).

The authors are grateful to A. I. Vaĭnshteĭn, E. G. Drukarev, and V. S. Polikanov for discussions.

¹The wave functions of electrons in other shells with the principal quantum number n can be obtained from (3) by replacing η by η/n , applying to (3) the differential operator $\Gamma_{n/m}$ [⁵], and discarding terms of order $(\alpha Z)^2$. The amplitude of the processes involving such electrons is obtained by applying this operator to the amplitude of the process involving the K-electron.

²It is not difficult to verify that in this case we discard terms of orders $\eta/m = \alpha Z$ and $\eta^2/2m\omega$.

³We derived the expression (16) for the amplitude A also by computing one Feynman diagram of the form shown in Fig. 1a with the wave functions and the electron Green function taken in the Furry-Sommerfeld-Maue [^{1,9}] approximation, and subsequently expanding the result in powers of αZ . To test the correctness of the computations, we also verified whether the amplitude (16) satisfies the condition of gauge invariance.

¹A. I. Akhiezer and V. B. Berestetskiĭ, *Kvantovaya Élektrodinamika (Quantum Electrodynamics)*, Nauka 1969, pp. 382, 371 (Eng. Transl., Interscience, New York, 1965).

²F. E. Low, *Phys. Rev.* **96**, 1428 (1954); M. Gell-Mann and M. L. Goldberger, *Phys. Rev.* **96**, 1433 (1954).

³V. G. Gorshkov, A. I. Mikhailov, V. S. Polikanov, and S. G. Sherman, *Phys. Lett.* **A30**, 455 (1969).

⁴M. Gavrilă and A. Costescu, *Phys. Rev.* **A2**, 1752 (1970); *Phys. Lett* **A28**, 614 (1969).

⁵V. G. Gorshkov and V. S. Polikanov, *ZhETF Pis. Red.* **9**, 464 (1969) [*JETP Lett.* **9**, 279 (1969)].

⁶C. Fronsdal, *Phys. Rev.* **179**, 1513 (1969).

⁷B. A. Zon, L. N. Manakov, and L. P. Rapoport, *Zh. Eksp. Teor. Fiz.* **56**, 400 (1969) [*Sov. Phys.-JETP* **29**, 220 (1969)].

⁸V. G. Gorshkov, A. I. Mikhailov, and V. S. Polikanov, *Nucl. Phys.* **55**, 273 (1964).

⁹V. G. Gorshkov, *Zh. Eksp. Teor. Fiz.* **47**, 1984 (1964) [*Sov. Phys.-JETP* **20**, 1331 (1965)].

¹⁰V. G. Gorshkov, *Materialy 7 shkoly LIYaF (Proceedings of the 7th LIYaF College)* Vol. 2, 415, 1972; E. G. Drukarev, *Yad. Fiz.* **17**, 342 (1973) [*Sov. J. Nucl. Phys.* **17**, 174 (1973)].

Translated by A. K. Agyei
124